The influence of pressure on crude oil biodegradation in shallow and deep Gulf of Mexico sediments

Uyen T. Nguyen[1]☯*, **Sara A. Lincoln**[1]☯, **Ana Gabriela Valladares Juárez**[2]☯, **Martina Schedler**[2]☯, **Jennifer L. Macalady**[1]‡, **Rudolf Müller**[2]‡, **Katherine H. Freeman**[1]‡

1 Department of Geosciences, The Pennsylvania State University, University Park, Pennsylvania, United States of America, **2** Institute of Technical Biocatalysis, Hamburg University of Technology, Hamburg, Germany

☯ These authors contributed equally to this work.
‡ These authors also contributed equally to this work.
* unguyen.psu.edu@gmail.com

Abstract

A significant portion of oil released during the Deepwater Horizon disaster reached the Gulf of Mexico (GOM) seafloor. Predicting the long-term fate of this oil is hindered by a lack of data about the combined influences of pressure, temperature, and sediment composition on microbial hydrocarbon remineralization in deep-sea sediments. To investigate crude oil biodegradation by native GOM microbial communities, we incubated core-top sediments from 13 GOM sites at water depths from 60–1500 m with crude oil under simulated aerobic seafloor conditions. Biodegradation occurred in all samples and followed a predictable compound class sequence dictated by molecular weight and structure. 45 to ~100% of total n-alkane and 3 to 60% of total polycyclic aromatic hydrocarbons (PAH) were depleted. In reactors incubated at 4°C and at pressures of 6–15 MPa, the depletion in total n-alkane was inversely correlated to pressure ($R^2 \sim 0.85$), equivalent to a 4% decrease in total n-alkane depletion for every 1 MPa increase. Our results indicated a modest inhibitory effect of pressure on biodegradation over our experimental range. However, the expansion of oil exploration to deeper waters (e.g., 5000 m) opens the risk of spills at conditions at which pressure might have a more pronounced effect.

Introduction

The 2010 Deepwater Horizon (DWH) blowout created the first major oil spill in deep waters. It released ~5 million barrels of Macondo oil to the Gulf of Mexico (GOM) at a water depth of 1500 m. An estimated 3–31% of the oil was transported to the seafloor, contaminating a region of 3200 km² around the Macondo wellhead [1, 2]. Oil sedimentation was promoted by marine oil snow formation and flocculent accumulation ("MOSSFA") [3, 4] which created oil-particle aggregates able to sink from surface waters or from the deep intrusion layers that formed in the water column at depths of 1000–1300 m [5]. These subsurface oil plumes, rather than oil

that reached surface waters, were considered a major source of oil to the seafloor, based on evidence of minimal photodegradation in oiled sediment samples [2]. Sinking high-density oil residues [6] and diffusion through the water column [7] may also have contributed to oil sedimentation.

Little information about the fate of oil spilled in deep-sea environments was available before the Deepwater Horizon blowout, and it was unclear how much could be extrapolated from studies of previous spills in very different environments (e.g. Exxon Valdez [8] and Gulf War [9]). Biodegradation is expected to be the major depletion mechanism of oil in deep, dark waters [10], where other common weathering processes in surface waters such as photooxidation and evaporation are not active. This expectation was reinforced by studies that revealed the enrichment of indigenous oil-degrading microbes and upregulation of hydrocarbon-degrading genes in deep waters following the spill [11–14]. Additionally, Stout & Payne [15] and Bagby et al. [16] found a significant depletion in various Macondo compound classes in deep (1000–1912 m) GOM sediments over the 4 years following the spill, indicating that indigenous microbial communities of the deep sea actively degrade oil components.

Deep sea environments, characterized by low temperature and high hydrostatic pressure, present energetic challenges to microbial metabolism. Among interconnected factors (e.g., physical conditions, nutrient and oxygen levels, background organic matter, and microbial community composition) that likely control hydrocarbon biodegradation on the seafloor [17, 18], the influence of pressure is least studied. Laboratory incubation experiments [19–25] have demonstrated that some bacteria are capable of hydrocarbon degradation under elevated pressure, but the effect of pressure in these studies has been mixed. Schwarz et al. [19, 20] discovered a 10 x decrease in rates of growth and hexadecane utilization of a microbial culture isolated from 4940-meter-deep sediments in the Atlantic Ocean at 50 MPa compared to the same culture incubated at ambient pressure (0.1 MPa). Grossi et al. [23] conversely, found no inhibitory effect of pressure on the growth and hexadecane consumption of piezotolerant, alkane-degrading *Marinobacter hydrocarbonoclasticus* strain #5 at 35 MPa. While 15 MPa slightly inhibited *Rhodococcus qingshengii TUHH-12* growth on *n*-hexadecane, it completely halted *Sphingobium yanoikuyae B1* growth on naphthalene [25]. In the first experimental study of the effect of pressure on oil degradation using environmental samples containing mixed microbial assemblages, Prince, Nash, and Hill [26] found that crude oil biodegradation by a surface water inoculum was 33% slower at 15 MPa than at surface pressure (0.1 MPa).

The expansion of oil exploration and production to deeper marine environments increases the likelihood of deep-sea oil spills. However, laboratory studies of the effect of pressure on hydrocarbon biodegradation have only focused on the fate of individual oil model compounds (e.g., hexadecane and naphthalene) or of crude oil in the water column. Biodegradation occurring in the water column, however, might not represent that in sediments, owing to potential differences between the two systems such as microbial concentration and access to hydrocarbon substrates. In this work, we investigated the rate and extent of crude oil biodegradation in sediments from the Northern GOM, collected at water depths from 62–1520 m, with a specific focus on the role of pressure. We approximated in-situ temperatures and pressures of sediments in 18-day incubation experiments with crude oil and examined changes in gas chromatography (GC)—amenable hydrocarbons. This is the first comparative study of crude oil biodegradation by indigenous microbes in sediments under deep and shallow marine conditions, designed to assess the potential for natural attenuation of spilled oil in GOM sediments.

Materials and methods

Incubation experiments

Thirteen sediment cores were collected in the Northern Gulf of Mexico (GOM) at water depths ranging from 62 to 1520 m, using a multicorer (Ocean Instruments MC-800) deployed from the R/V WeatherBird II ship, in August 2014. Sampling area spanned from 28˚49'36" N to 29˚53'56" N and from 86˚17'40" W to 89˚30'48" W (Fig 1, Table 1). Field area was not on any private land, no permissions were required for collecting sediment cores at these sites and this study did not involve endangered or protected species. Approximately 0.2 g of coretop (0–4 mm) sediment from each site were amended with 5 µL autoclaved sweet Louisiana crude, a Macondo oil surrogate, and 5 mL of minimal mineral medium following DSMZ methanogenium medium 141 recipe [25, 27] and vortexed. Incubation conditions approximated in-situ physical environments of the sediments: pressure ranged from 0.1 to 15 MPa and temperatures were 4, 10, and 20˚C. For each sediment site, we incubated oil-amended sediment in duplicate, with a parallel control of un-amended sediment. An oil-amended control was frozen to -20˚C immediately after shaking and was used to determine the initial extractable oil composition. Sediments were incubated at pressures ranging from 0.1 to 15.3 MPa, selected in order to approximate *in situ* pressures for the sample (Table 1). Incubation vials in > 0.1 MPa experiments were placed in stainless steel reactors that were capped with bronze lids and pressurized with nitrogen gas [28]. Incubation vials in ambient pressure experiments (0.1 MPa) were placed in equivalent aluminum reactors. In addition, to further explore the effects of pressure,
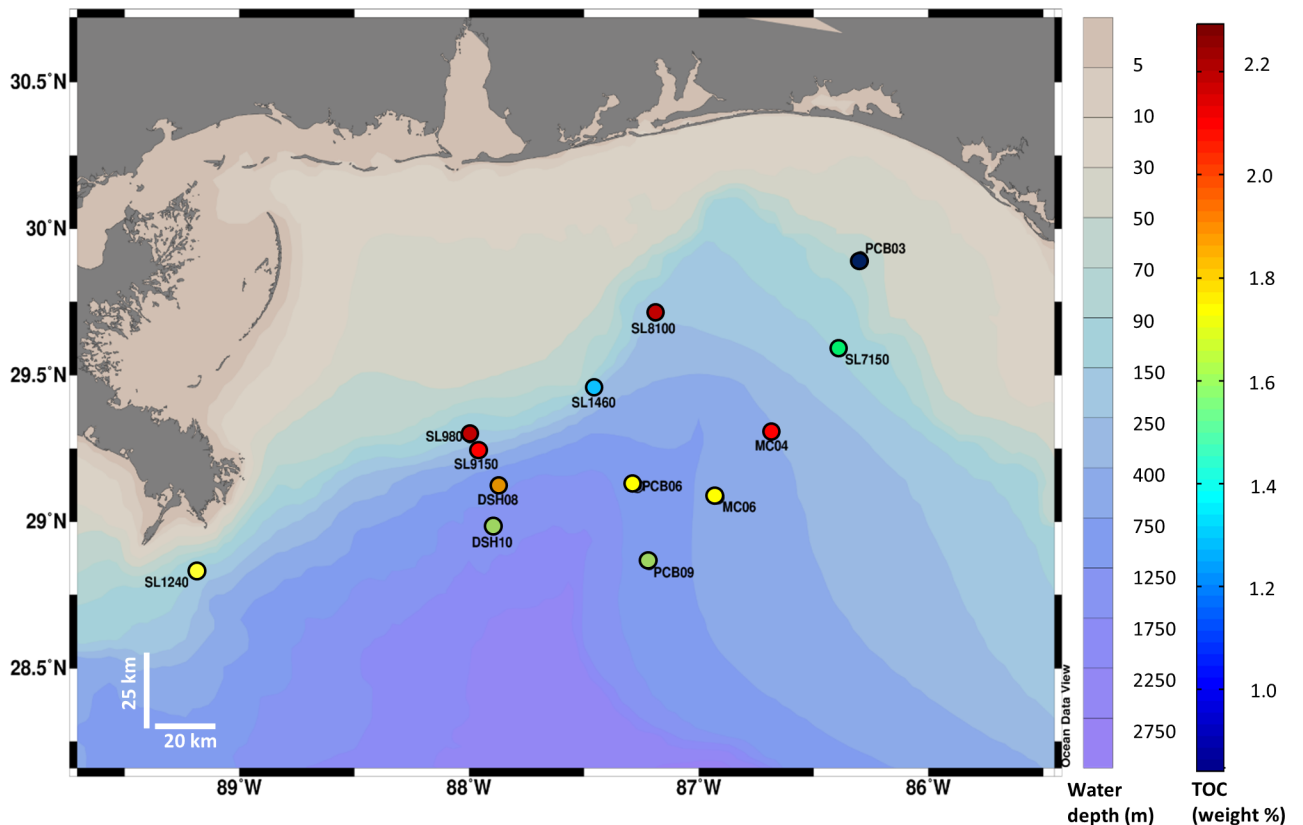
Fig 1. Map of sampling sites. Locations of 13 sampling sites across the Northern Gulf of Mexico at water depth ranging from 60–1520m. Circles are color-coded representing total organic content (TOC, percent weight of sediments). Schlitzer, R., Ocean Data View, http://odv.awi.de, 2016.

https://doi.org/10.1371/journal.pone.0199784.g001

Table 1. Physical conditions of sediment sites and laboratory incubation conditions. (CTD: conductivity-temperature-depth device, P: pressure, T: temperature).

Site	Water depth (m)	Latitude	Longitude	CTD bottom water T (˚C)	CTD bottom water oxygen (µmol/kg)	Incubation P initial (MPa)	Incubation P final (MPa)	Incubation T (˚C)	Comments
SL1240	62	28 49.592	89 30.796	20.71	129.26	0.1	0.1	20	**Incubation conditions approximated in situ pressure and temperature conditions**
PCB03	96	29 53.935	86 17.68	18.33	126.77	0.1	0.1	20	
SL980	150	29 17.513	88 02.512	16.08	118.28	2.5	2.5	20	
SL7150	196	29 35.231	86 22.84	10.91	111.6	1.9	1.8	10	
SL1460	212	29 27.348	87 26.994	18.28	126.69	2.5	2.1	20	
SL8100	226	29 42.428	87 11.338	11.04	109.52	1.9	1.9	10	
SL9150	251	29 14.957	87 59.750	11.12	118.76	2.5	2.3	10	
MC04	399	29 18.44	86 40.495	9.42	112.55	4.0	3.6	10	
MC06	595	29 5.013	86 54.871	7.26	124.08	5.8	5.4	4	
PCB09	981	28 51.548	87 12.888	5.22	165.33	10.5	9.4	4	
PCB06	1008	29 07.371	87 15.928	5.18	165.86	9.4	8.7	4	
DSH08	1127	29 07.378	87 52.091	4.83	176.5	11.1	10.5	4	
DSH10	1520	28 58.687	87 53.438	5.07	169.4	15.28	14.08	4	
PCB06	1008	29 07.371	87 15.928	5.18	165.86	0.1	0.1	4	**Ambient pressure replicates of the three deepest sites**
DSH08	1127	29 07.378	87 52.091	4.83	176.5	0.1	0.1	4	
DSH10	1520	28 58.687	87 53.438	5.07	169.4	0.1	0.1	4	

three deep sediment samples were incubated both at high pressures (9.4, 11.1, and 15.3 MPa) and at 0.1 MPa and 4˚C. Because core-top sediments were relatively well-oxygenated *in situ* (Table 1), all experiments were carried out under aerobic conditions. Incubation vials were stirred at 200 rpm with magnets to keep oxygen, sediments, and nutrients well-mixed over the course of the incubation period. Experiments were stopped after 18 days and frozen at -20˚C until analysis.

Organic extraction and analysis

Total organic content (TOC) of core-top sediments was measured as weight percent carbon of sediment using a Leco C/S-744 analyzer after sediments were treated with hydrochloric acid 1N to remove inorganic carbon. Incubation vials were centrifuged to separate aqueous and solid phases in order to measure the water fraction and sediment-associated oil components. Any visible oil on vial walls after decanting was recovered with additional sea water medium and transferred to the water fraction (WAF). For each sample, both phases were extracted with an azeotrope of dichloromethane and methanol (in a proportion of 9:1 by volume) three times. Liquid phases (~5 mL) were extracted with a total of 15 mL, while sediments (~ 0.2 g) were extracted with a total volume of 10 mL solvent. Organic extracts were separated into

aliphatic, aromatic, and polar fractions by silica gel chromatography using 100% *n*-hexane, *n*-hexane and dichloromethane (4:1, v/v), and dichloromethane and methanol (4:1, v/v)), respectively, as eluents (S1 Fig). The aliphatic and aromatic fractions, represented in the first and second eluted fractions, were analyzed on a Trace 1310 gas chromatography (GC) coupled to an ISQ LT single quad mass spectrometer (MS) (Thermo Scientific) (S1 Appendix). Polycyclic aromatic hydrocarbons (PAHs) in the aromatic fraction were further characterized on an Agilent HP 6890 GC coupled to a HP 5973 mass selective detector in selected ion monitoring (SIM) mode due to the higher peak resolution on this system (S1 and S2 Tables). *N*-alkane and branched alkanes were quantified using an alkane standard mix of C_7-C_{40} solution (Sigma-Aldrich). Parent PAHs and their alkylated homologues were quantified using a standard mix of 16 EPA priority PAH (Sigma-Aldrich) (S1 Appendix).

Biodegradation parameters

To characterize and quantify biodegradation effects on oil components, we normalized compounds to internal biomarkers generally considered to be recalcitrant [29–31]. Aliphatic compounds were normalized to $17\alpha(H),21\beta(H)$-hopane (C_{30} hopane, detected and quantified with m/z 191) and aromatic compounds were normalized to C_{26} triaromatic sterane (C_{26} TAS, detected and quantified with m/z 231), both of which were abundant in the amended oil. The relative loss of different compound classes was calculated as following (t_0 and t_f are the initial and final time points for the incubation):

$$\text{Total n–alkane loss (\%)} = \left[1 - \left. \frac{\left[\frac{\sum n-alkane}{C30\ hopane} \right]_{tf}}{\left[\frac{\sum n-alkane}{C30\ hopane} \right]_{t0}} \right. \right] * 100 \qquad (1)$$

$$\text{Total PAH loss (\%)} = \left[1 - \left. \frac{\left[\frac{\sum PAH}{C26\ TAS} \right]_{tf}}{\left[\frac{\sum PAH}{C26\ TAS} \right]_{t0}} \right. \right] * 100 \qquad (2)$$

We defined total *n*-alkanes as the sum of C_{15-40} *n*-alkanes and total PAH as the sum of all PAHs analyzed (S1 Table). We also determined ratios of biomarker abundances that are commonly used in petroleum biodegradation studies such as C_{17} *n*-alkane/pristane, C_{18} *n*-alkane/phytane, ΣC_{15-20} *n*-akane/ΣC_{15-40} *n*-alkane, and isomer ratios of mono-methylated PAH [32].

Results and discussion

Biodegradation sequence

Compound loss patterns after incubation followed the canonical biodegradation sequence [31–34] and were consistent with field data on Macondo oil degradation [15, 16]. The loss sequence was governed by molecular weights and structures; short chain alkanes were degraded to a greater extent than long chain alkanes (S2 Fig), and straight chain *n*-alkanes were preferentially degraded over their saturated isoprenoid analogues (Fig 2). Long chain *n*-alkanes up to C_{40} were degraded, suggesting that these long alkanes were more susceptible to biodegradation than C_{30} hopane; these results contrast with those reported by Bagby et al., who used C_{40} *n*-alkane as conservative tracer due to its recalcitrance in biodegradation [16]. Total PAH decreased to a smaller extent than total n-alkanes, with the resistance to biodegradation increased with the number of rings and the degree of alkylation. For instance, 3-ring PAHs including phenanthrene and its alkylated homologues were depleted in most samples,
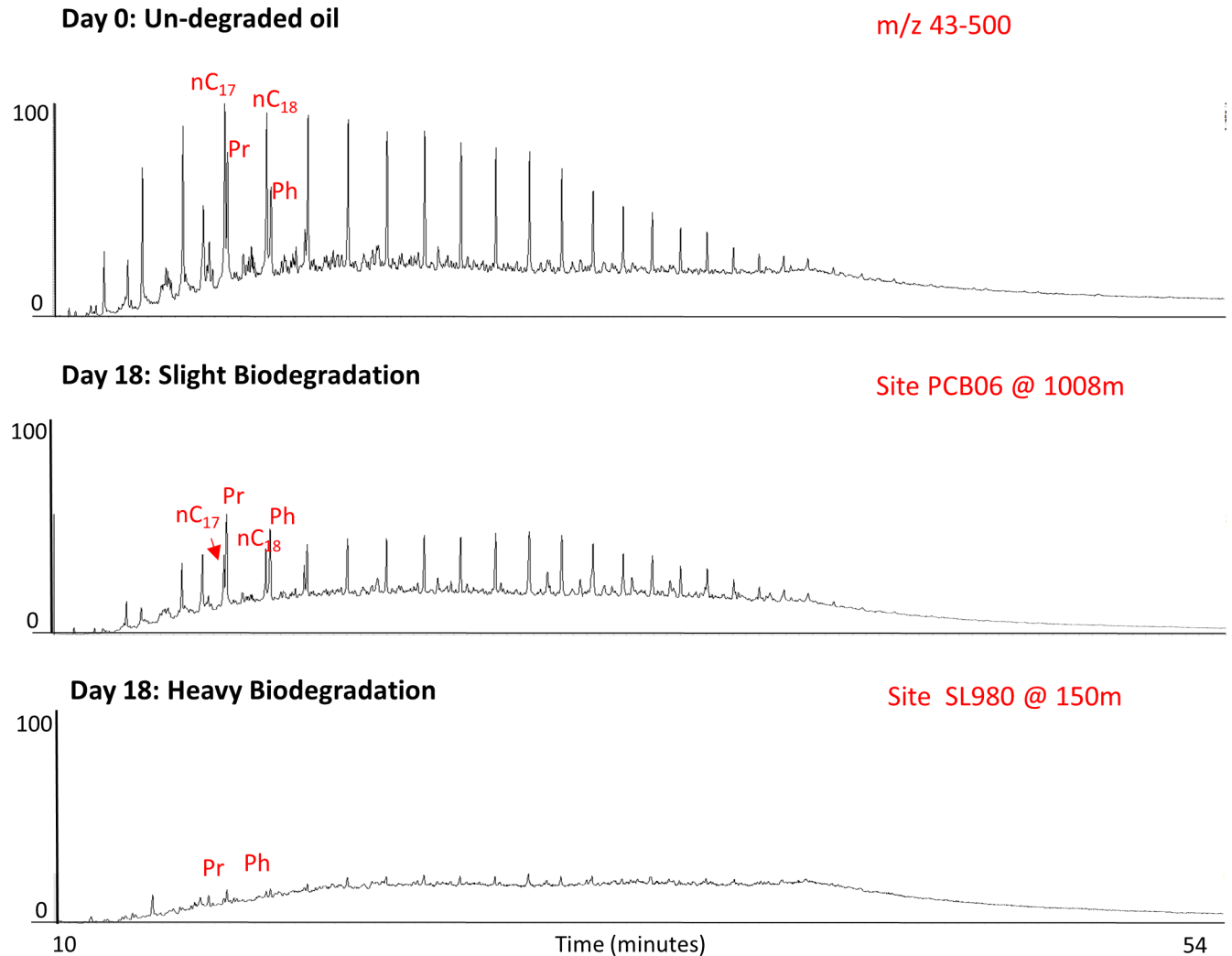
Fig 2. Chromatograms of crude oil biodegradation. Examples of total ion chromatograms of oil extract (normalized to C_{30} hopane) from two extremes of biodegradation at different water depths (nC17 = C17 *n*-alkane, nC18 = C18 *n*-alkane, Pr = Pristane, Phy = Phytane).

whereas 4-ring PAHs such as pyrene and chrysene were only slightly degraded in the most degraded samples (S3 Fig).

We used C_{30} hopane and C_{26} TAS as conservative oil biomarkers in our analyses. Compound groups such as hopanes, steranes, and TAS have been widely used as conservative tracers for oil, based on the assumption that they are relatively recalcitrant [29–31]. However, recent laboratory studies [35–37] and field data [15, 16] have shown that these compounds can be more subject to biodegradation than previously thought. We justified the treatment of C_{30} hopane and C_{26} TAS as conservative tracers in our study for two reasons. First, our incubation duration (18 days) was shorter than the time scales of hopane and sterane biodegradation observed in the field [38] and experimentally. Homohopane biodegradation in laboratory experiments was reported to begin after 3–5 weeks at 30˚C [35–36], while no degradation of TAS occurred over 21 days of oil incubation at 37˚C [39]. Second, our experiments showed no change in ratios of R/S isomers of homohopane series (S2 Appendix), as is usually observed during biodegradation of these biomarkers [40–43].

Alkane degradation and pressure inhibitory effect

After 18 days, total *n*-alkanes were depleted in all samples. The percent loss of total alkanes ranged from 40% to 100%, and samples incubated at lower pressures (< 5 MPa) had more than 80% alkane depletion. Replicate incubations exhibited a small range of variability, with standard deviations from 0.03 to 5% (S3 Table). The extent of biodegradation was greater at shallower sites than at deeper sites (p < 0.05, one tailed *t*-test, Figs 2 and 3A, Table 2). Degradation of oil in both sediment and water fractions were relatively similar at each site. For all samples incubated at higher pressures (i.e., from 5.8 to 15 MPa, at 4˚C), total *n*-alkane loss was inversely proportional to pressure ($r^2 > 0.85$). This linear relationship represents ~ 4% decrease in the rate of alkane loss via biodegradation per 1 MPa increase, assuming simple first order kinetics (Fig 3B). The rate of *n*-alkane loss was slowest in samples incubated at 15 MPa, and ~ 36% less than in their counterparts incubated at 0.1 MPa and ~ 55% slower than samples incubated at 0.1 to 2.5 MPa from other sediment sites.

We calculated mean half-lives (assuming a first-order rate law) for total *n*-alkane to be ~ 21 days at 15.3 MPa, and ~ 9 days at 0.1–2.5 MPa. Our results are consistent with those of Prince, Nash, and Hill [26] who observed a 33% reduction in degradation rate at 15 MPa compared to 0.1 MPa, using a water column inoculum amended with 3 ppm oil. We also found inverse relationships between loss via biodegradation and water depth for other aliphatic compounds, including cyclohexanes, pristane, and phytane (S4 and S5 Figs).

PAH degradation

Overall, total PAH concentrations decreased as much as 60% after incubations, and standard deviations averaged 19% between replicates from each site (S3 Table). There was no significant difference between shallow and deep sediments (p > 0.05, one tailed *t*-test, Table 2). Sediments from the shallowest water depths (incubated at 0.1 MPa) only exhibited limited PAH biodegradation. Samples incubated at 2.5 MPa showed the greatest extent of PAH depletion, consistent with having the greatest *n*-alkanes degradation. High pressure samples (9.4–15 MPa) also showed decreases in total PAHs, though to a smaller extent than at 2.5MPa. Depletion of total PAHs at 15 MPa (~ 35%) was comparable to PAH depletion in samples incubated at 2.5 MPa. This was surprising since the 15 MPa sample showed the least n-alkane depletion. This led us to consider the potential for an experimental artifact due to loss of volatile compounds during sample decompression following the incubation period. Indeed, when this is accounted for, we observed a trend toward greater PAH loss at lower pressures (Fig 4A and S6 Fig). To estimate the effect of off-gassing, we used ratios of methylated homologues of phenanthrene (MP), fluorene (MF), and dibenzothiophene (MDBT). Biodegradation of hydrocarbons is often isomer-specific. Isomers may share similar physicochemical properties yet be more or less susceptible to biodegradation [34, 44–46], possibly due to enzyme specificity or steric considerations. At low pressures (2.5 MPa), samples with high levels of preferential degradation of certain methylated PAH isomers was consistent with previous published studies. For instance, we detected a decrease in the ratio of 1-MP/9-MP in degraded samples at 2.5 MPa, which is consistent with 9-methylphenanthrene (9-MP) being the most resistant to microbial oxidation among all MP isomers [47]. In contrast, this ratio remained relatively constant in 15 MPa samples, indicating both compounds, which have similar vapor pressures, were loss during de-gassing to the same extent. Similar consistency of ratios was observed for (2-MDBT+3-MDBT)/(1-MDBT+4-MDBT) and 4-MF/1-MF (Fig 4B). Attributing all PAH loss at 15 MPa (~ 35%) to off-gassing, we calculated that off-gassing only accounted for a maximum of ~ 3.5% loss in total n-alkane depletion at 15 MPa (out of a total loss of ~ 42%) (S3 Appendix). Thus, we concluded that biodegradation was indeed the major cause for n-alkane depletion at 15 MPa.
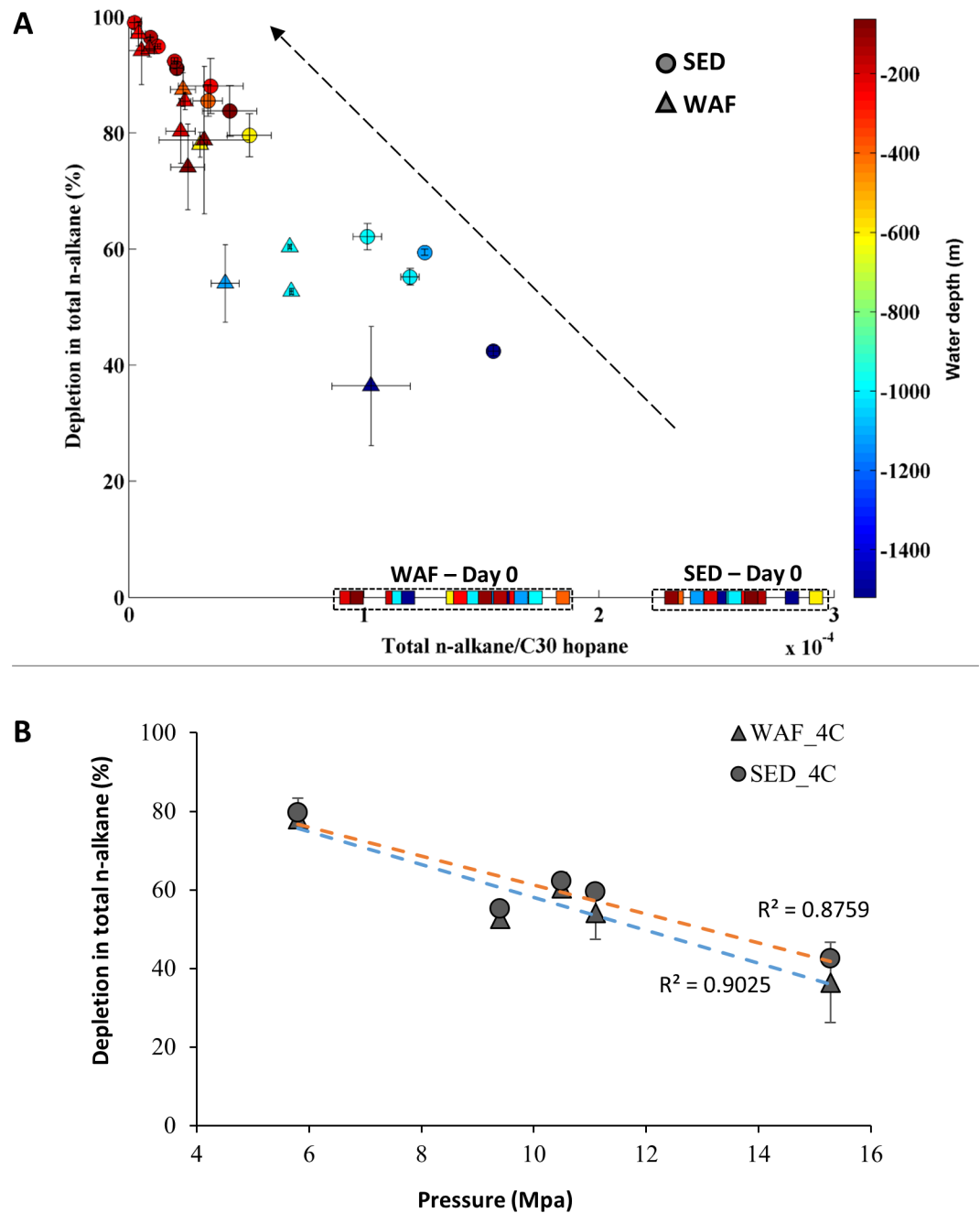
Fig 3. Total n-alkane degradation. Depletion of total *n*-alkane (%) after 18 days of incubation in both water fraction (WAF, triangles) and sediment fraction (SED, circles), the dashed arrow is interpreted as the direction of increasing biodegradation extent: A, All samples: Initial total *n*-alkanes are represented by squares. Samples are color-coded according to sampling water depths and B, Inhibitory effect of pressure on n-alkane biodegradation at 4˚C. Error bars represent one standard deviations from the means.

Factors controlling biodegradation

Even before anthropogenic influence, the GOM seafloor was subject to petroleum input via natural seeps (average of 140,000 tons of petroleum annually) [48], which have likely been active over millions of years. Continued exposure may have primed GOM microbial

Table 2. Comparison in biodegradation of *n*-alkanes and PAHs between shallow (< 500 m) and deep (> 500 m) sediments.

Group by depth	*n*-alkane–SED (%)	*n*-alkane–WAF (%)	PAH–SED (%)	PAH–WAF (%)
< 500 m	91.4 ± 5.1	73.6 ± 14.6	33.5 ± 25	29.8 ± 15.8
> 500 m	62.4 ± 12.5	45.6 ± 17.4	34.5 ± 19.9	27.4 ± 9.1
t-test p value	0.00007	0.001	0.92	0.64

Mean ± one standard deviation of depletion percent in total *n*-alkane and total PAH, and p values for one tailed *t*-tests with significant level α = 0.05 (SED: sediment fraction, WAF: water fraction).

https://doi.org/10.1371/journal.pone.0199784.t002

communities to develop the capability to readily degrade hydrocarbons. Prior exposure to hydrocarbons could accelerate biodegradation, as a memory response [49]. We speculated that our sediments were previously exposed to oil, based on the presence of background oil hydrocarbons including *n*-alkanes and C_{30} hopane (S4 Appendix). In fact, several sites are within the area impacted by Macondo oil, including the three deepest water sites (DSH08, DSH10, and PCB06) [2, 16, 50]. This might explain the promptness in degrading oil of the GOM sediments seen in our study.

The level of hydrocarbon contamination in sediments has been proposed to influence rates of biodegradation [16, 51, 52]. In our study, oil amendment led to an average concentration of 1.1 μg C_{30}-hopane/g sediment (S5 Appendix). This equates to a state of "heavy oil contamination" as defined by Valentine et al. (2014), who used a threshold of >750 ng/g in GOM sediments [2]. Samples at 2.5 MPa showed extensive biodegradation (~100% Σn-alkanes, ~60% ΣPAHs depletion after 18 days) despite having similar heavy contamination level as deep sites, suggesting that contamination level was not a direct inhibitory factor, and that other factors such as nutrient and oxygen concentration, and microbial community composition might be more important rate-limiting forces.

There are inevitable challenges in isolating the effect of pressure on biodegradation. In previous studies of pressure effects, single inocula were incubated under both high and low pressure; either sea surface inocula were introduced to high pressure [26] or piezotolerant strains were placed in ambient pressure [19, 20]. Introducing microbes to non-native conditions can impact their growth and carbon utilization [53–55]. In this study, we attempted to minimize this concern by comparing the hydrocarbon-degrading capacity of native sediment communities under approximated in-situ conditions (although our sediments were exposed to surface conditions for a period after sampling). Given possible compromising factors deep-sea microbial communities encountered during sampling and experimental setup, we recognize that our results may provide a conservative estimation of biodegradation at high pressure.

To better understand the impact incubation under non-native conditions might have, we incubated three deep GOM sediments at both in situ seafloor (9.4–15 MPa) and atmospheric pressure. Hydrocarbon degradation in these high and low pressure treatments of the same sediments appeared to be stochastic. The DSH10 sample showed more extensive n-alkane biodegradation at surface pressure (0.1 MPa) than at seafloor pressure (15 MPa), consistent with an inhibitory effect of pressure. Conversely, the DSH08 sediment showed much less n-alkane degradation at surface pressure than at seafloor pressure (11 MPa). The PCB06 sample, however, showed virtually no difference in biodegradation between surface and seafloor pressure (9.4 MPa) treatments (Table 3). The absence of a clear trend in this subset of our data may be the result of pressure-induced perturbation in sediment community. We conclude that, until technology for in-situ deep sea incubation [56, 57] or pressure-retaining sampling [58, 59] becomes more widely available, the best practice for hydrocarbon biodegradation studies is to incubate samples under conditions simulating their native, in-situ environments.
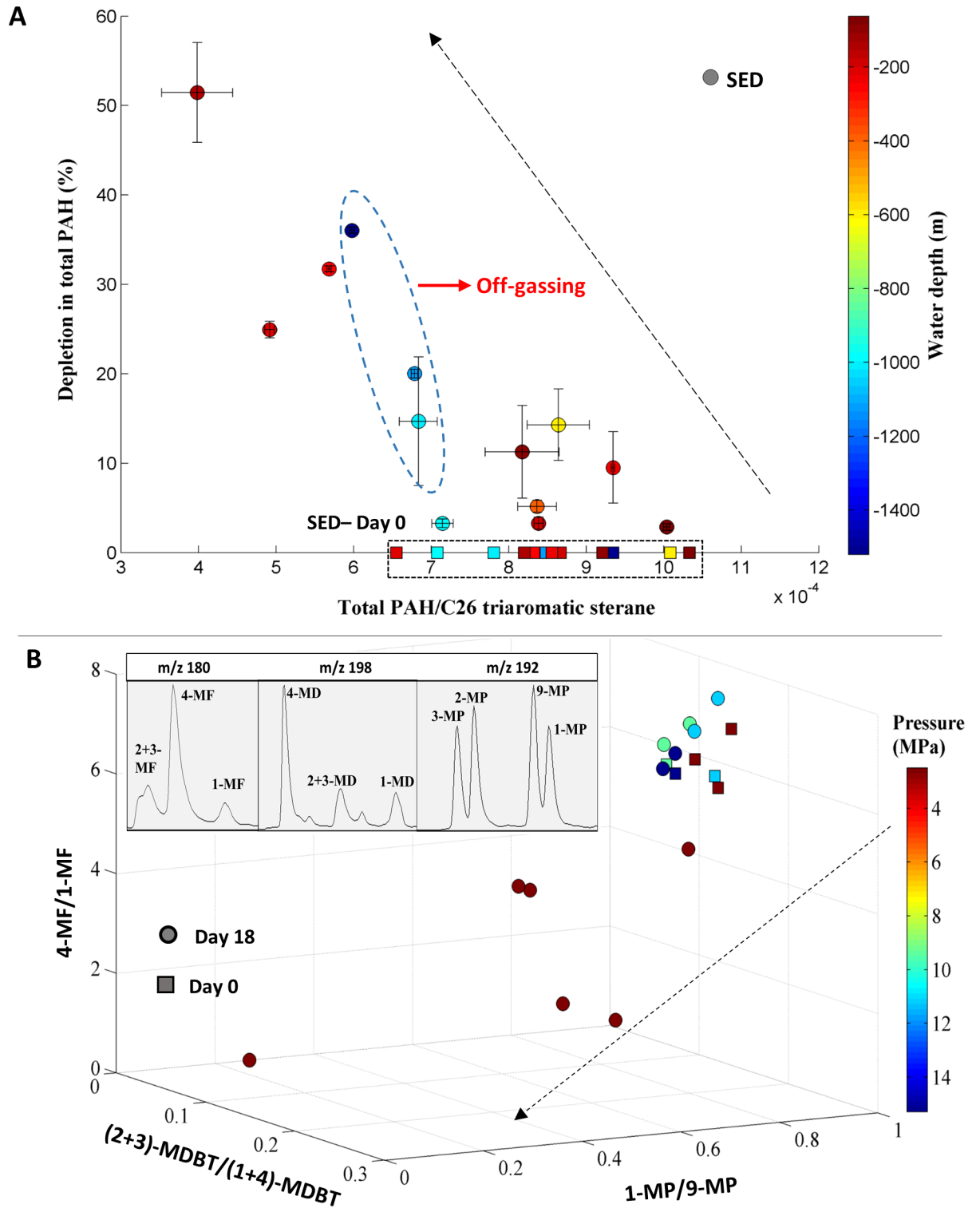
Fig 4. PAH degradation. Depletion of total PAH (%) of crude oil in sediment fraction (SED, circles) at after 18 days of incubation. The dashed arrow is interpreted as the direction of increasing biodegradation extent. A, All samples: Initial total PAHs are represented by squares. Samples are color-coded according to sampling water depths. Depletion in deep water samples are possibly due to off-gassing effect. B, Distinguishing biodegradation from off-gassing, using different isomer ratios of methylated-PAHs (MF: methyl fluorene *m/z* 180; MD: methyldibenzothiophene *m/z* 198; MP: methylphenanthrene *m/z* 192). Samples are color coded by pressures (MPa). Error bars represent one standard deviations from the means.

Table 3. Comparison of total *n*-alkane depletion percent (mean ± one standard deviation) between high in-situ pressure incubation of the three deepest sites and their ambient pressure (0.1Mpa) incubation counterparts.

Sample	In-situ water depth (m)	Total *n*-alkane depletion (%)	
		In-situ Pressure	Surface pressure
DSH10	1520	42.5 ± 0.92	66.5 ± 0.57
DSH08	1127	59.5 ± 0.55	12.05 ± 6.5
PCB06	1008	55.2 ± 1.44	46.9 ± 3

https://doi.org/10.1371/journal.pone.0199784.t003

Conclusions

Our study assessed the rate and nature of oil biodegradation across the Northern GOM at a wide water depth range (60–1520 m), representing a range of shallow water to approximately the depth of DWH spill. All sediments were found to degrade oil. Piezotolerant microbial cultures at pressure up to 15 MPa demonstrated their capability to degrade oil, suggesting a high potential for natural attenuation of spilled oil. Under optimal nutrients and oxygen availability, as provided here, we predict that it would take a minimum of 42 days for complete n-alkane degradation at 15 MPa, compared to average of 19 days at shallow sites (0.1–2.5 MPa), assuming first order kinetics. Our study focused on the early, oxic biodegradation of GC-amenable oil, after 18 days of incubation. However, we expect that if the experiments were left to run longer on the scale of months or years with sufficient oxygen and nutrient supply, biodegradation could extend to other compound classes such as >4-ring PAHs and biomarkers (e.g., hopanes, steranes). Although pressure alone was not a major inhibitor of biodegradation in our experimental range, the expansion of oil exploration to deeper waters (e.g., 5000 m) opens the risk of spills at conditions at which pressure might have a more significant effect.

Supporting information

S1 Appendix. Gas chromatography–Mass spectrometry (GC-MS) and quantification methods.
(DOCX)

S2 Appendix. Distribution of hopanes and triaromatic sterane compound groups, showing the similarity between day 0 and day 18 samples, to justify the use of C30 hopane and C26-TAS as internal conservative oil biomarker in our study.
(DOCX)

S3 Appendix. Calculation of *n*-alkane depletion due to off-gassing at 15 Mpa.
(DOCX)

S4 Appendix. Background hydrocarbons in un-incubated sediments.
(DOCX)

S5 Appendix. Calculating contamination level.
(DOCX)

S1 Table. Oil hydrocarbons analyzed in this study and their quantitative molecular ion (*m/z*).
(DOCX)

S2 Table. Selected Ion Monitoring method for alkylated PAHs. Each compound group is identified based on a quantitative ion and a confirmation ion *m/z* (Zeigler et al., 2008; Robbat Jr. and Wilton, 2014*). * Zeigler C., MacNamara K., Wang Z., Robbat Jr. A. Total alkylated

polycyclic aromatic hydrocarbon characterization and quantitative comparison of selected ion monitoring versus full scan gas chromatography/mass spectrometry based on spectral deconvolution. Journal of Chromatography A 2008; 1205, 109–116. Robbat Jr., A.; Wilton, N.M. A new spectral deconvolution–Selected ion monitoring method for the analysis of alkylated polycyclic aromatic hydrocarbons in complex mixtures. Talanta 2014 125, 114–124.
(DOCX)

S3 Table. Depletion (%) of total n-alkane and total PAH of individual samples. (TOC: total organic carbon, Carb: carbonate in the sediments, P: pressure, T: temperature, WD: water depth, SED: sediment fraction, WAF: water fraction).
(DOCX)

S1 Fig. Summary of experimental and analytical procedures.
(TIF)

S2 Fig. Depletion of different *n*-alkanes to compare the extent of biodegradation as number of carbon increases. A. Mean and standard errors plot for depletion of each *n*-alkane for all day-18 samples; B. Boxplot for depletion of each n-alkane for all day-18 samples.
(TIFF)

S3 Fig. Depletion of different PAH compound groups to compare the extent of biodegradation as number of rings increases. (C1: methyl, C2: ethyl or dimethyl, C3: trimethyl, C4: tetramethyl; Naph: napthalene, PNT: phenanthrene, Fluo: fluorene, DBT: dibenzothiophene, Py: pyrene, 11H-benzoF: 11H-benzo[b]fluorene, Chy: chrysene).
(TIFF)

S4 Fig. Depletion in total cyclohexanes (m/z 83) after 18 days. The dashed arrow represents interpreted direction of increasing biodegradation extent.
(TIF)

S5 Fig. Change in ratios of C_{17} n-alkane/pristane and C_{18} n-alkane/phytane after 18 days. A, sediment fractions (SED) and B, water fractions (WAF). Initial ratios are represented by the black square. Samples are color-coded according to sampling water depths. The dashed arrow represents interpreted direction of increasing biodegradation extent.
(TIF)

S6 Fig. Depletion of total PAHs after 18 days of incubation of oil in water fraction (WAF, triangles). Initial total PAHs are represented by squares. Samples are color-coded according to sampling water depths. The dashed arrow represents interpreted direction of increasing biodegradation extent.
(TIF)

Acknowledgments

Author Contributions

Conceptualization: Sara A. Lincoln, Ana Gabriela Valladares Juárez, Martina Schedler, Jennifer L. Macalady, Rudolf Müller, Katherine H. Freeman.

Data curation: Uyen T. Nguyen.

Formal analysis: Uyen T. Nguyen.

Funding acquisition: Katherine H. Freeman.

Investigation: Uyen T. Nguyen.

Methodology: Uyen T. Nguyen, Sara A. Lincoln, Ana Gabriela Valladares Juárez, Martina Schedler, Jennifer L. Macalady, Rudolf Müller, Katherine H. Freeman.

Project administration: Sara A. Lincoln.

Supervision: Sara A. Lincoln, Katherine H. Freeman.

Validation: Uyen T. Nguyen, Sara A. Lincoln, Ana Gabriela Valladares Juárez, Martina Schedler.

Visualization: Uyen T. Nguyen.

Writing – original draft: Uyen T. Nguyen, Sara A. Lincoln.

Writing – review & editing: Uyen T. Nguyen, Sara A. Lincoln, Ana Gabriela Valladares Juárez, Martina Schedler, Rudolf Müller, Katherine H. Freeman.

References

1. Chanton J., Zhao T., Rosenheim B.E., Joye S., Bosman S., Brunner C., et al. Using Natural Abundance Radiocarbon To Trace the Flux of Petrocarbon to the Seafloor Following the Deepwater Horizon Oil Spill. *E*nviron. Sci. Technol. 2015, 49 (2), pp 847–854.

2. Valentine D.L., Fisher G.B., Bagby S.C., Nelson R.K., Reddy C.M., Sylva S.P., et al. Fallout plume of submerged oil from Deepwater Horizon. Proc Natl Acad Sci. 2014, 111(45): 15906–1591. https://doi.org/10.1073/pnas.1414873111 PMID: 25349409

3. Passow U., Ziervogel K., Asper V., Diercks A. Marine snow formation in the aftermath of the Deepwater Horizon spill in the Gulf of Mexico. Environ Res Lett 2012, 7(3).

4. Daly K.L., Passow U., Chanton J., and Hollander D.J. Assessing the impacts of oil-associated marine snow formation and sedimentation during and after the Deepwater Horizon oil spill. Anthropocene 201613:18–33.

5. McNutt M.K., Camilli R., Crone T.J., Guthrie G.D., Hsieh P.A., Ryerson T.B., et al. Review of flow rate estimates of the Deepwater Horizon oil spill. Proc Natl Acad Sci USA 2012, 109(50):20260–20267.

6. Stevens C.C., Thibodeaux L.J., Overton E.B., Valsaraj K.T., Nandakumar K., Rao A., et al. Sea Surface Oil Slick Light Component Vaporization and Heavy Residue Sinking: Binary Mixture Theory and Experimental Proof of Concept. Environmental Engineering Science 2015, 32(8).

7. Tkalich P., Huda K., HoongGin K.Y. A multiphase oil spill model. J. Hydraul.Res. 2003, 41, 115–125.

8. Gibeaut J.C., Piper E. Shoreline Oiling Assessment of the Exxon Valdez Oil Spill. EVOS Restoration Project Final Report 93038 1993, Exxon Valdez Trustee Council: Anchorage, AK.

9. Hayes M.O., Al-Mansi A.M., Jensen J.R., Narumalani S., Aurand Don V., Al-Momen A., et al. Distribution of oil from the Gulf War spill within intertidal habitats—one year later. Proceedings of the 1993 Oil Spill Conf. 1993, pp. 373–381. American Petroleum Institute, Washington, DC.

10. Scoma A, Yakimov M.M, Boon N. Challenging Oil Bioremediation at Deep-Sea Hydrostatic Pressure. Front. Microbiol. 2016, 7:1203.

11. Hazen T.C, Dubinsky E.A., DeSantis T.Z., Andersen G.L., Piceno Y.M., Singh N., et al. Deep-Sea Oil Plume Enriches Indigenous Oil-Degrading Bacteria. Science 2010, 330(6001): 204–208. https://doi.org/10.1126/science.1195979 PMID: 20736401

12. Bælum J, Borglin S, Chakraborty R, Fortney JL, Lamendella R, Mason OU, et al. Deep-sea bacteria enriched by oil and dispersant from the Deepwater Horizon spill. Environ Microbiol. 2012, 14: 2405–2416. doi: https://doi.org/10.1111/j.1462-2920.2012.02780.x PMID: 22616650

13. Redmond M.C., Valentine D.L. Natural gas and temperature structured a microbial community response to the Deepwater Horizon oil spill. Proc Natl Acad Sci USA 2012, 109(50): 20292–20297. https://doi.org/10.1073/pnas.1108756108 PMID: 21969552

14. Lu Z., Deng Y., VanNostrand J.D., He Z., Voordeckers J., Zhou A., et al. Microbial gene functions enriched in the Deepwater Horizon deep-sea oil plume. ISME J. 2012, 6: 451–460.

15. Stout S.A., Payne J. R. Macondo oil in deep-sea sediments: Part 1 –sub-sea weathering of oil deposited on the seafloor. Marine Pollution Bulletin 2016, 111, 365–380.

16. Bagby S.C., Reddy C.M., Aeppli C., Fisher G.B., and Valentine D.L. Persistence and biodegradation of oil at the ocean floor following Deepwater Horizon. Proc Natl Acad Sci USA 2017, 114(1): E9–E18. https://doi.org/10.1073/pnas.1610110114 PMID: 27994146

17. Leahy J.G., Colwell R.R. Microbial degradation of hydrocarbons in the environment. Microbiol Rev. 1990, 54(3):305–315.

18. Swannell R.P., Lee K., McDonagh M. Field evaluations of marine oil spill bioremediation. Microbiol Rev. 1996, 60(2):342–365. PMID: 8801437

19. Schwarz J.R., Walker J.D., Colwell R.R. Deep sea bacteria: growth and utilization of hydrocarbons at ambient and in situ pressure Applied Microbiology 1974, p. 982–986.

20. Schwarz J.R., Walker J.D., Colwell R.R. Deep-sea bacteria: growth and utilization of n-hexadecane at in situ temperature and pressure. Canadian Journal of Microbiology 1975, 21(5): 682–687.

21. Bazylinski D.A., Wirsen C.O., Jannasch H.W. Microbial utilization of naturally occurring hydrocarbons at the Guaymas Basin hydrothermal vent site. Appl Environ Microbiol. 1989, 55(11): 2832–6. PMID: 16348045

22. Cui Z., Lai Q., Dong C., Shao Z. Biodiversity of polycyclic aromatic hydrocarbon-degrading bacteria from deep sea sediments of the Middle Atlantic Ridge. Environ. Microbiol. 2008, 10: 2138–2149. https://doi.org/10.1111/j.1462-2920.2008.01637.x PMID: 18445026

23. Grossi V., Yakimov M.M., Al Ali B., Tapilatu Y., Cuny P., Goutx M., et al. Hydrostatic pressure affects-membrane and storage lipid compositions of the piezotolerant hydrocarbon-degrading Marinobacter hydrocarbonoclasticus strain# 5. Environ. Microbiol. 2010, 12, 2020–2033.

24. Tapilatu Y., Acquaviva M., Guigue C., Miralles G., Bertrand J.-C., Cuny P. Isolation of alkane-degrading bacteria from deep-sea Mediterranean sediments. Letters in Applied Microbiology 2010 50: 234–236.

25. Schedler M., Hiessl R., Valladares Juárez A.G., Gust G., Müller R. Effect of high pressure on hydrocarbon-degrading bacteria. AMB Express 2014, 4:7.

26. Prince R.C., Nash G.W, Hill S.J. The biodegradation of crude oil in the deep ocean. Marine Pollution Bulletin 2016.

27. DSMZ GmbH (2012a) 141 METHANOGENIUM MEDIUM., http://www.dsmz.de/microorganisms/medium/pdf/DSMZ_Medium141.pdf.

28. Valladares Júarez A.G., Kadimesetty H.S., Achatz D.E., Schedler M., and Müller R. Online Monitoring of Crude Oil Biodegradation at Elevated Pressures. IEEE 2015, 8(2).

29. Butler E.L., Douglas G.S., Steinhauer W.S., Prince R.C., Aczel T., Hsu C.S., et al. Hopane, a New Chemical Tool for Measuring Oil Biodegradation. In book: On-Site Bioreclamation: Processes for Xeno-biotic and Hydrocarbon Treatment 1991, pp.515–521, Butterworth-Heinemann, Boston.

30. Prince R.C., Elmendorf D.L, Lute J.R, Hsu C.S, Haith C.E, Senius J.D, et al. 17α(H),21β(H)-Hopane as a Conserved Internal Marker for Estimatlng the Biodegradation of Crude Oil. Environ. Sci. Technol. 1994, 28, 142–145.

31. Wenger L.M, Davis C.L, Isaksen G.H. Multiple Controls on Petroleum Biodegradation and Impact on Oil Quality. SPE Reservoir Evaluation & Engineering 2002, 5: 375–383.

32. Wang Z., Fingas M. Development of oil hydrocarbon fingerprinting and identification techniques. Marine Pollution Bulletin 2003, 47: 423–452.

33. Peters K. E., Moldowan J. W. The Biomarker Guide: Interpreting Molecular Fossils in Petroleum and Ancient Sediments. Prentice Hall: New York 1993.

34. Wang Z., Fingas M., Blenkinsopp M., Sergy G., Landriault M., Sigouin L, et al. Comparison of oil composition changes due to biodegradation and physical weathering in different oils. J. Chromatogr. 1998, A 809: 89–1107.

35. Bost F.D., Frontera-Suau R., McDonald T.J., Peters K.E., Morris P.J. Aerobic biodegradation of hopanes and norhopanes in Venezuelan crude oils. Organic Geochemistry 2001, 32(1): 105–114.

36. Frontera-Suau R., Bost F.D., McDonald T.J., Morris P.J. Aerobic biodegradation of hopanes and other biomarkers by crude oil-degrading enrichment cultures. Environ. Sci. Technol. 2002, 36: 4585–4592.

37. Chen L., Xiao C., Luo X., Sun W. Study on biological degradation and transform characteristics of different components in petroleum hydrocarbon used by bacterial consortium. Environ Earth Sci. 2016, 75: 816.

38. Atlas R., and Bragg J. Assessing the long-term weathering of petroleum on shorelines: uses of conserved components for calibrating loss and bioremediation potential. Arctic and Marine Oilspill Program Technical Seminar (Canada) 2007, 263–289.

39. Wang C., Chen B., Zhang B., Guo P., Zhao M. Study of weathering effects on the distribution of aromatic steroid hydrocarbons in crude oils and oil residues. Environ. Sci.: Processes Impacts 2014, 16: 2408–2414.

40. Requejo A. G., Halpern H. I. An unusual hopane biodegradation sequence in tar sands from the Pt Arena (Monterey) Formation. Nature 1989, 342: 670–673.

41. Moldowan J.M., McCaffrey M.A. A novel microbial hydrocarbon degradation pathway revealed by hopane demethylation in a petroleum reservoir. Geochimica et Cosmochimica Acta. 1995, 59(9): 1891–1894.

42. Peters K.E., Moldowan J.M., McCaffrey M.A., Fago F.J. Selective biodegradation of extended hopanes to 25-norhopanes in petroleum reservoirs. Insights from molecular mechanics. Organic Geochemistry 1996, 24(8):765–783.

43. Watson J. S., Jones D. M., Swannell R. P. J. and van Duin A. C. T. Formation of carboxylic acids during aerobic biodegradation of crude oil and evidence of microbial oxidation of hopanes. Organic Geochemistry 2002, 33(10): 1153–1169.

44. Rogoff M. H., Wender I. Methylnaphthalene oxidations by pseudomonads. J. Bacteriol. 1958, 77: 783–788.

45. Bao J., Zhu C. The effects of biodegradation on the compositions of aromatic hydrocarbons and maturity indicators in biodegraded oils from Liaohe Basin. Science in China Series D: Earth Sciences 2009, 52: 59–68.

46. Vila J and Grifoll M. Actions of *Mycobacterium* sp. Strain AP1 on the Saturated- and Aromatic-Hydrocarbon Fractions of Fuel Oil in a Marine Medium. Appl. Environ. Microbiol. 2009, 75(19): 6232–6239. https://doi.org/10.1128/AEM.02726-08 PMID: 19666730

47. Rowland S. J., Alexander R., Kagi R. I., Jones D. M., Douglas A. G. Microbial degradation of aromatic compounds of crude oils: A coMParison of laboratory and field observations. Org. Geochem. 1986, 9: 153–161.

48. National Research Council (US) Committee on Oil in the Sea: Inputs, Fates, and Effects. Oil in the Sea III: Inputs, Fates, and Effects. Washington (DC): National Academies Press (US) 2003.

49. Hazen T.C., Prince R.C., Mahmoudi N. Marine Oil Biodegradation. Environ. Sci. Technol. 2016, 50, 2121−2129.

50. Romero I.C., Schwing P.T., Brooks G.R., Larson R.A., Hastings D.W., Ellis G., et al. Hydrocarbons in Deep-Sea Sediments following the 2010 Deepwater Horizon Blowout in the Northeast Gulf of Mexico. PLoS ONE 2015, 10(5): e0128371. https://doi.org/10.1371/journal.pone.0128371 PMID: 26020923

51. Short J.W., Irvine G.V., Mann D.H., Maselko J.M., Pella J.J., Lindeberg M.R., et al. Slightly weathered Exxon Valdez oil persists in Gulf of Alaska beach sediments after 16 years. Environ Sci Technol. 2007, 41(4):1245–50.

52. Del'Arco J.P., De França F.P. Influence of oil contamination levels on hydrocarbon biodegradation in sandy sediment. Environ Pollut. 2001, 112(3):515–519.

53. ZoBell C. E. Bacterial life in the deep sea. Bull. Misaki Mar. Biol. Inst. Kyoto Univ. 1968, 12:77–96.

54. Seki H., Robinson D. Effect of Decompression on Activity of Microorganisms in Seawater. Int. Rev. Gesamter. Hydrobiol. 1969, 54: 201–205.

55. Jannasch H.W., Wirsen C.O. Microbial activities in undecompressed and decompressed deep-Seawater samples. Appl.Environ.Microbiol. 1982, p.1116–1124.

56. Orcutt B.N., Bach W., Becker K., Fisher A.T., Hentscher M., Toner B.M., et al. Colonization of subsurface microbial observatories deployed in young ocean crust. ISME J. 2011, 5(4):692–703. https://doi.org/10.1038/ismej.2010.157 PMID: 21107442

57. Smith A., Popa R., Fisk M. R., Nielsen M., Wheat C. G., Jannasch H. W. *In situ* enrichment of ocean crust microbes on igneous minerals and glasses using an osmotic flow-through device. Geochem. Geophys. Geosyst. 2011, 12:Q06007.

58. Jannasch H.W., Wirsen C.O. Retrieval of concentrated and undecompressed microbial populations from the deep sea. Appl.Environ.Microbiol. 1977, 33: 642–646.

59. Smedile F., Cono V.L., Genovese M., Ruggeri G., Denaro R., Crisafi F., et al. High Pressure Cultivation of Hydrocarbonoclastic Aerobic Bacteria. Hydrocarbon and Lipid Microbiology Protocols. Springer Protocols Handbooks 2017, 33–49.